



Zero-Drift, Single-Supply, Rail-to-Rail Input/Output Operational Amplifiers

AD8551/AD8552/AD8554

FEATURES

- Low Offset Voltage: 1 μV
- Input Offset Drift: 0.005 $\mu\text{V}/^\circ\text{C}$
- Rail-to-Rail Input and Output Swing
- +5 V/+2.7 V Single-Supply Operation
- High Gain, CMRR, PSRR: 130 dB
- Ultralow Input Bias Current: 20 pA
- Low Supply Current: 700 $\mu\text{A}/\text{Op Amp}$
- Overload Recovery Time: 50 μs
- No External Capacitors Required

APPLICATIONS

- Temperature Sensors
- Pressure Sensors
- Precision Current Sensing
- Strain Gage Amplifiers
- Medical Instrumentation
- Thermocouple Amplifiers

GENERAL DESCRIPTION

This new family of amplifiers has ultralow offset, drift and bias current. The AD8551, AD8552 and AD8554 are single, dual and quad amplifiers featuring rail-to-rail input and output swings. All are guaranteed to operate from +2.7 V to +5 V single supply.

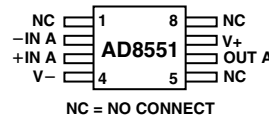
The AD855x family provides the benefits previously found only in expensive autozeroing or chopper-stabilized amplifiers. Using Analog Devices' new topology these new zero-drift amplifiers combine low cost with high accuracy. No external capacitors are required.

With an offset voltage of only 1 μV and drift of 0.005 $\mu\text{V}/^\circ\text{C}$, the AD8551 is perfectly suited for applications where error sources cannot be tolerated. Temperature, position and pressure sensors, medical equipment and strain gage amplifiers benefit greatly from nearly zero drift over their operating temperature range. The rail-to-rail input and output swings provided by the AD855x family make both high-side and low-side sensing easy.

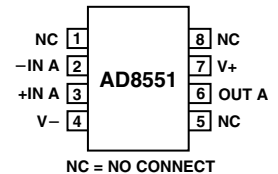
The AD855x family is specified for the extended industrial/automotive (-40°C to $+125^\circ\text{C}$) temperature range. The AD8551 single is available in 8-lead MSOP and narrow 8-lead SOIC packages. The AD8552 dual amplifier is available in 8-lead narrow SO and 8-lead TSSOP surface mount packages. The AD8554 quad is available in narrow 14-lead SOIC and 14-lead TSSOP packages.

PIN CONFIGURATIONS

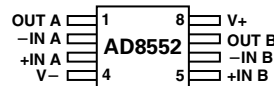
8-Lead MSOP
(RM Suffix)



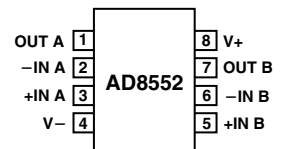
8-Lead SOIC
(R Suffix)



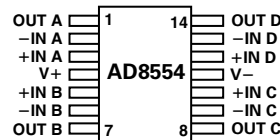
8-Lead TSSOP
(RU Suffix)



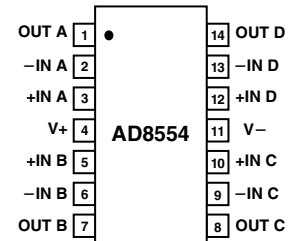
8-Lead SOIC
(R Suffix)



14-Lead TSSOP
(RU Suffix)



14-Lead SOIC
(R Suffix)



REV. A

Information furnished by Analog Devices is believed to be accurate and reliable. However, no responsibility is assumed by Analog Devices for its use, nor for any infringements of patents or other rights of third parties that may result from its use. No license is granted by implication or otherwise under any patent or patent rights of Analog Devices. Trademarks and registered trademarks are the property of their respective companies.

One Technology Way, P.O. Box 9106, Norwood, MA 02062-9106, U.S.A.
Tel: 781/329-4700 www.analog.com
Fax: 781/326-8703 © 2002 Analog Devices, Inc. All rights reserved.

AD8551/AD8552/AD8554—SPECIFICATIONS

ELECTRICAL CHARACTERISTICS ($V_S = +5\text{ V}$, $V_{CM} = +2.5\text{ V}$, $V_O = +2.5\text{ V}$, $T_A = +25^\circ\text{C}$ unless otherwise noted)

Parameter	Symbol	Conditions	Min	Typ	Max	Units
INPUT CHARACTERISTICS						
Offset Voltage	V_{OS}	$-40^\circ\text{C} \leq T_A \leq +125^\circ\text{C}$		1	5	μV
Input Bias Current	I_B	$-40^\circ\text{C} \leq T_A \leq +125^\circ\text{C}$		10	50	pA
Input Offset Current	I_{OS}	$-40^\circ\text{C} \leq T_A \leq +125^\circ\text{C}$		1.0	1.5	nA
Input Voltage Range				20	70	pA
Common-Mode Rejection Ratio	CMRR	$V_{CM} = 0\text{ V to }+5\text{ V}$ $-40^\circ\text{C} \leq T_A \leq +125^\circ\text{C}$	0	150	200	pA
Large Signal Voltage Gain ¹	A_{VO}	$R_L = 10\text{ k}\Omega$, $V_O = +0.3\text{ V to }+4.7\text{ V}$ $-40^\circ\text{C} \leq T_A \leq +125^\circ\text{C}$	120	140	5	dB
Offset Voltage Drift	$\Delta V_{OS}/\Delta T$	$-40^\circ\text{C} \leq T_A \leq +125^\circ\text{C}$	115	130		dB
			120	135		dB
				0.005	0.04	$\mu\text{V}/^\circ\text{C}$
OUTPUT CHARACTERISTICS						
Output Voltage High	V_{OH}	$R_L = 100\text{ k}\Omega$ to GND $-40^\circ\text{C to }+125^\circ\text{C}$	4.99	4.998		V
			4.99	4.997		V
		$R_L = 10\text{ k}\Omega$ to GND $-40^\circ\text{C to }+125^\circ\text{C}$	4.95	4.98		V
			4.95	4.975		V
Output Voltage Low	V_{OL}	$R_L = 100\text{ k}\Omega$ to V+ $-40^\circ\text{C to }+125^\circ\text{C}$		1	10	mV
				2	10	mV
		$R_L = 10\text{ k}\Omega$ to V+ $-40^\circ\text{C to }+125^\circ\text{C}$		10	30	mV
				15	30	mV
Short Circuit Limit	I_{SC}	$-40^\circ\text{C to }+125^\circ\text{C}$	± 25	± 50		mA
Output Current	I_O	$-40^\circ\text{C to }+125^\circ\text{C}$		± 40		mA
				± 30		mA
				± 15		mA
POWER SUPPLY						
Power Supply Rejection Ratio	PSRR	$V_S = +2.7\text{ V to }+5.5\text{ V}$ $-40^\circ\text{C} \leq T_A \leq +125^\circ\text{C}$	120	130		dB
			115	130		dB
Supply Current/Amplifier	I_{SY}	$V_O = 0\text{ V}$ $-40^\circ\text{C} \leq T_A \leq +125^\circ\text{C}$		850	975	μA
				1,000	1,075	μA
DYNAMIC PERFORMANCE						
Slew Rate	SR	$R_L = 10\text{ k}\Omega$		0.4		$\text{V}/\mu\text{s}$
Overload Recovery Time				0.05	0.3	ms
Gain Bandwidth Product	GBP			1.5		MHz
NOISE PERFORMANCE						
Voltage Noise	e_n p-p	0 Hz to 10 Hz		1.0		$\mu\text{V p-p}$
	e_n p-p	0 Hz to 1 Hz		0.32		$\mu\text{V p-p}$
Voltage Noise Density	e_n	$f = 1\text{ kHz}$		42		$\text{nV}/\sqrt{\text{Hz}}$
Current Noise Density	i_n	$f = 10\text{ Hz}$		2		$\text{fA}/\sqrt{\text{Hz}}$

NOTE

¹Gain testing is highly dependent upon test bandwidth.

Specifications subject to change without notice.

ELECTRICAL CHARACTERISTICS ($V_S = +2.7\text{ V}$, $V_{CM} = +1.35\text{ V}$, $V_O = +1.35\text{ V}$, $T_A = +25^\circ\text{C}$ unless otherwise noted)

Parameter	Symbol	Conditions	Min	Typ	Max	Units
INPUT CHARACTERISTICS						
Offset Voltage	V_{OS}	$-40^\circ\text{C} \leq T_A \leq +125^\circ\text{C}$		1	5	μV
Input Bias Current	I_B	$-40^\circ\text{C} \leq T_A \leq +125^\circ\text{C}$		10	50	pA
Input Offset Current	I_{OS}	$-40^\circ\text{C} \leq T_A \leq +125^\circ\text{C}$		1.0	1.5	nA
Input Voltage Range		$-40^\circ\text{C} \leq T_A \leq +125^\circ\text{C}$		150	200	pA
Common-Mode Rejection Ratio	CMRR	$V_{CM} = 0\text{ V to }+2.7\text{ V}$ $-40^\circ\text{C} \leq T_A \leq +125^\circ\text{C}$	0	115	130	V dB
Large Signal Voltage Gain ¹	A_{VO}	$R_L = 10\text{ k}\Omega$, $V_O = +0.3\text{ V to }+2.4\text{ V}$ $-40^\circ\text{C} \leq T_A \leq +125^\circ\text{C}$	110	110	140	dB
Offset Voltage Drift	$\Delta V_{OS}/\Delta T$	$-40^\circ\text{C} \leq T_A \leq +125^\circ\text{C}$		105	130	dB
				0.005	0.04	$\mu\text{V}/^\circ\text{C}$
OUTPUT CHARACTERISTICS						
Output Voltage High	V_{OH}	$R_L = 100\text{ k}\Omega$ to GND $-40^\circ\text{C to }+125^\circ\text{C}$	2.685	2.697		V
		$R_L = 10\text{ k}\Omega$ to GND $-40^\circ\text{C to }+125^\circ\text{C}$	2.685	2.696		V
		$R_L = 10\text{ k}\Omega$ to GND $-40^\circ\text{C to }+125^\circ\text{C}$	2.67	2.68		V
Output Voltage Low	V_{OL}	$R_L = 100\text{ k}\Omega$ to V+ $-40^\circ\text{C to }+125^\circ\text{C}$		2.67	2.675	V
		$R_L = 100\text{ k}\Omega$ to V+ $-40^\circ\text{C to }+125^\circ\text{C}$		1	10	mV
		$R_L = 10\text{ k}\Omega$ to V+ $-40^\circ\text{C to }+125^\circ\text{C}$		2	10	mV
		$R_L = 10\text{ k}\Omega$ to V+ $-40^\circ\text{C to }+125^\circ\text{C}$		10	20	mV
Short Circuit Limit	I_{SC}	$-40^\circ\text{C to }+125^\circ\text{C}$	± 10	15	20	mV mA
Output Current	I_O	$-40^\circ\text{C to }+125^\circ\text{C}$		± 10		mA
		$-40^\circ\text{C to }+125^\circ\text{C}$		± 5		mA
POWER SUPPLY						
Power Supply Rejection Ratio	PSRR	$V_S = +2.7\text{ V to }+5.5\text{ V}$ $-40^\circ\text{C} \leq T_A \leq +125^\circ\text{C}$	120	130		dB
Supply Current/Amplifier	I_{SY}	$V_O = 0\text{ V}$ $-40^\circ\text{C} \leq T_A \leq +125^\circ\text{C}$	115	130		dB
				750	900	μA
				950	1,000	μA
DYNAMIC PERFORMANCE						
Slew Rate	SR	$R_L = 10\text{ k}\Omega$		0.5		$\text{V}/\mu\text{s}$
Overload Recovery Time				0.05		ms
Gain Bandwidth Product	GBP			1		MHz
NOISE PERFORMANCE						
Voltage Noise	e_n p-p	0 Hz to 10 Hz		1.6		$\mu\text{V p-p}$
Voltage Noise Density	e_n	$f = 1\text{ kHz}$		75		$\text{nV}/\sqrt{\text{Hz}}$
Current Noise Density	i_n	$f = 10\text{ Hz}$		2		$\text{fA}/\sqrt{\text{Hz}}$

NOTE

¹Gain testing is highly dependent upon test bandwidth.

Specifications subject to change without notice.

AD8551/AD8552/AD8554

ABSOLUTE MAXIMUM RATINGS¹

Supply Voltage	+6 V
Input Voltage	GND to $V_S + 0.3$ V
Differential Input Voltage ²	± 5.0 V
ESD(Human Body Model)	2,000 V
Output Short-Circuit Duration to GND	Indefinite
Storage Temperature Range	
RM, RU and R Packages	-65°C to +150°C
Operating Temperature Range	
AD8551A/AD8552A/AD8554A	-40°C to +125°C
Junction Temperature Range	
RM, RU and R Packages	-65°C to +150°C
Lead Temperature Range (Soldering, 60 sec)	+300°C

NOTES

¹Stresses above those listed under Absolute Maximum Ratings may cause permanent damage to the device. This is a stress rating only; functional operation of the device at these or any other conditions above those listed in the operational sections of this specification is not implied. Exposure to absolute maximum rating conditions for extended periods may affect device reliability.

²Differential input voltage is limited to ± 5.0 V or the supply voltage, whichever is less.

Package Type	θ_{JA} ¹	θ_{JC}	Units
8-Lead MSOP (RM)	190	44	°C/W
8-Lead TSSOP (RU)	240	43	°C/W
8-Lead SOIC (RN)	158	43	°C/W
14-Lead TSSOP (RU)	180	36	°C/W
14-Lead SOIC (RN)	120	36	°C/W

NOTE

¹ θ_{JA} is specified for worst case conditions, i.e., θ_{JA} is specified for device in socket for P-DIP packages, θ_{JA} is specified for device soldered in circuit board for SOIC and TSSOP packages.

ORDERING GUIDE

Model	Temperature Range	Package Description	Package Option	Brand ¹
AD8551ARM ²	-40°C to +125°C	8-Lead MSOP	RM-8	AHA
AD8551AR	-40°C to +125°C	8-Lead SOIC	RN-8	
AD8552ARU ³	-40°C to +125°C	8-Lead TSSOP	RU-8	
AD8552AR	-40°C to +125°C	8-Lead SOIC	RN-8	
AD8554ARU ³	-40°C to +125°C	14-Lead TSSOP	RU-14	
AD8554AR	-40°C to +125°C	14-Lead SOIC	RN-14	

NOTES

¹Due to package size limitations, these characters represent the part number.

²Available in reels only. 1,000 or 2,500 pieces per reel.

³Available in reels only. 2,500 pieces per reel.

CAUTION

ESD (electrostatic discharge) sensitive device. Electrostatic charges as high as 4000 V readily accumulate on the human body and test equipment and can discharge without detection. Although the AD8551/AD8552/AD8554 features proprietary ESD protection circuitry, permanent damage may occur on devices subjected to high energy electrostatic discharges. Therefore, proper ESD precautions are recommended to avoid performance degradation or loss of functionality.



Typical Performance Characteristics—AD8551/AD8552/AD8554

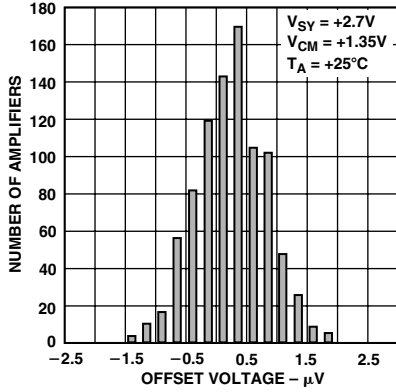


Figure 1. Input Offset Voltage Distribution at +2.7 V

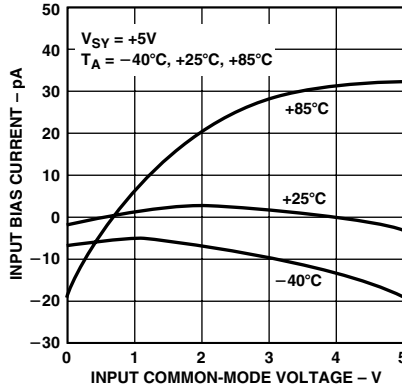


Figure 2. Input Bias Current vs. Common-Mode Voltage

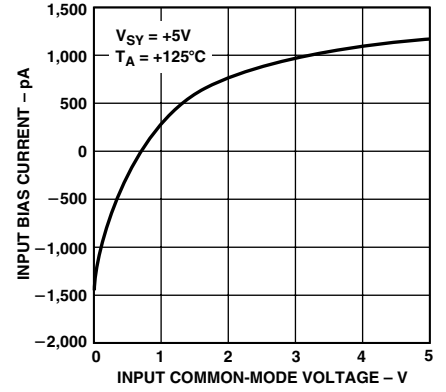


Figure 3. Input Bias Current vs. Common-Mode Voltage

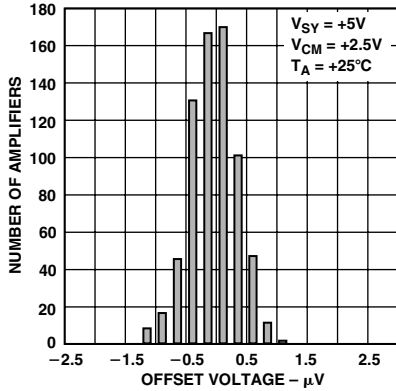


Figure 4. Input Offset Voltage Distribution at +5 V

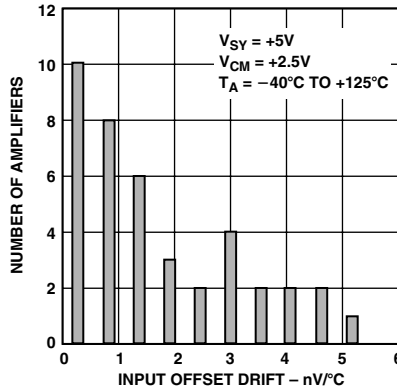


Figure 5. Input Offset Voltage Drift Distribution at +5 V

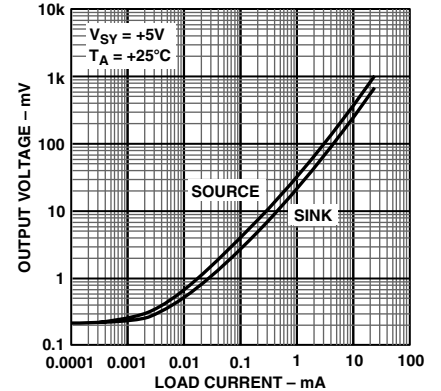


Figure 6. Output Voltage to Supply Rail vs. Output Current at +5 V

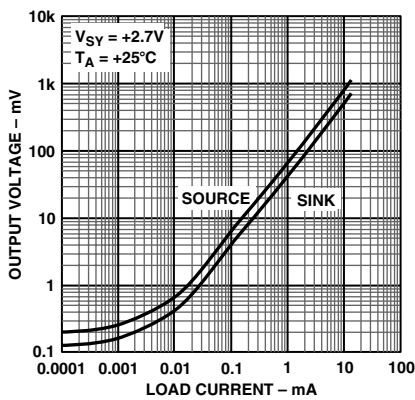


Figure 7. Output Voltage to Supply Rail vs. Output Current at +2.7 V

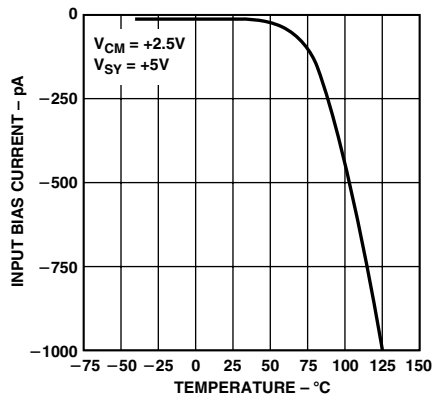


Figure 8. Bias Current vs. Temperature

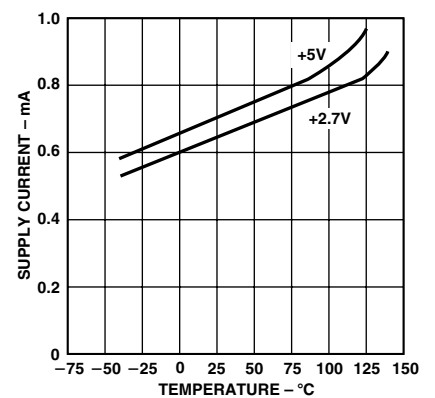


Figure 9. Supply Current vs. Temperature

AD8551/AD8552/AD8554

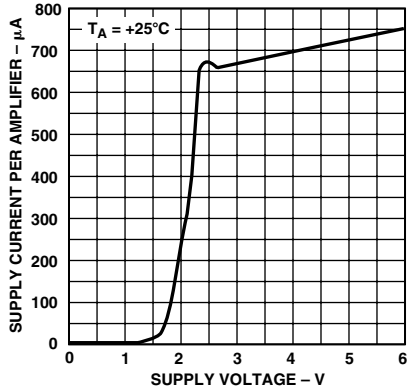


Figure 10. Supply Current vs. Supply Voltage

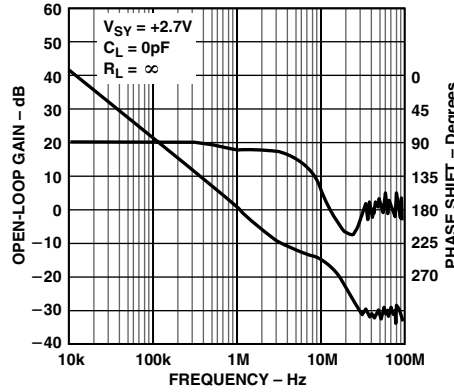


Figure 11. Open-Loop Gain and Phase Shift vs. Frequency at +2.7 V

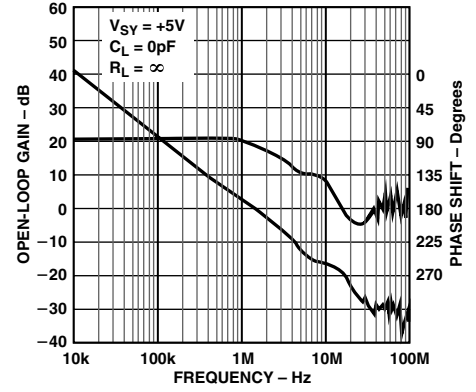


Figure 12. Open-Loop Gain and Phase Shift vs. Frequency at +5 V

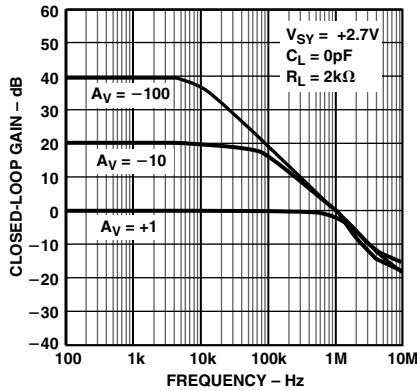


Figure 13. Closed Loop Gain vs. Frequency at +2.7 V

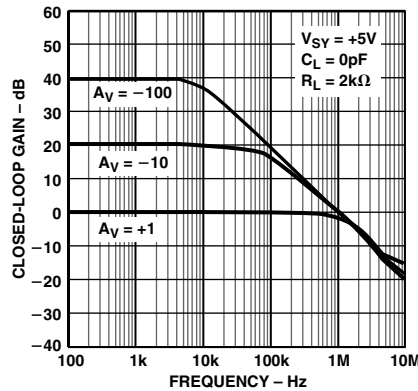


Figure 14. Closed Loop Gain vs. Frequency at +5 V

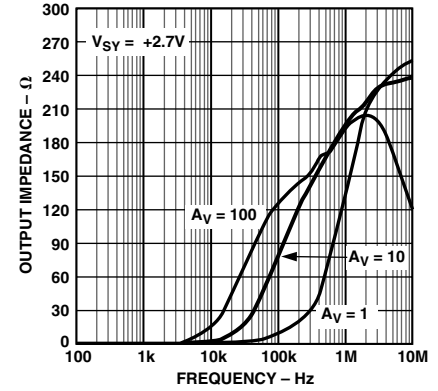


Figure 15. Output Impedance vs. Frequency at +2.7 V

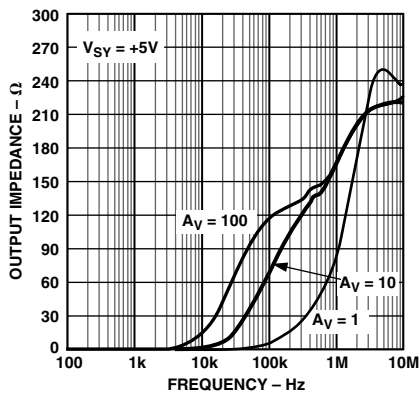


Figure 16. Output Impedance vs. Frequency at +5 V

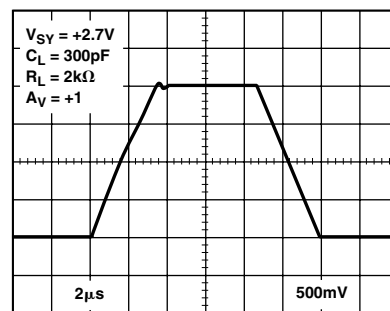


Figure 17. Large Signal Transient Response at +2.7 V

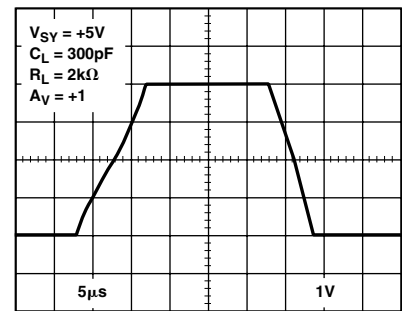


Figure 18. Large Signal Transient Response at +5 V

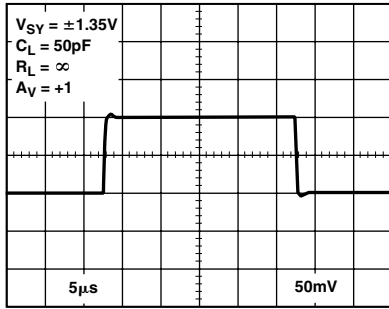


Figure 19. Small Signal Transient Response at +2.7 V

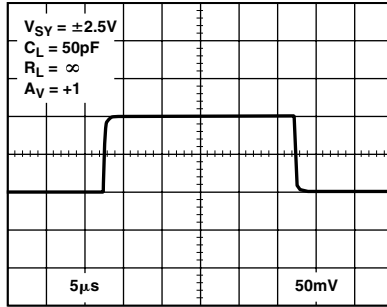


Figure 20. Small Signal Transient Response at +5 V

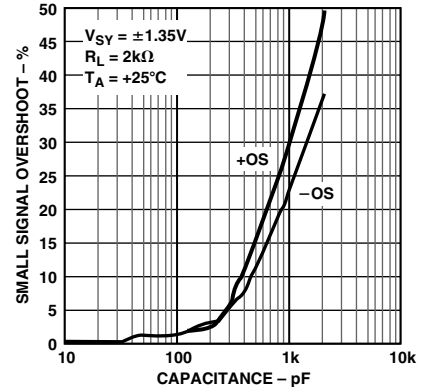


Figure 21. Small Signal Overshoot vs. Load Capacitance at +2.7 V

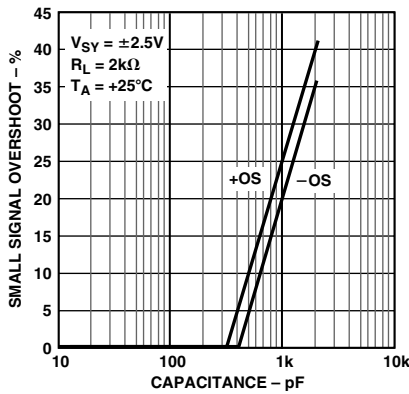


Figure 22. Small Signal Overshoot vs. Load Capacitance at +5 V

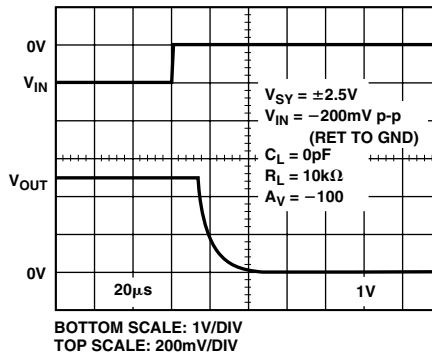


Figure 23. Positive Overvoltage Recovery

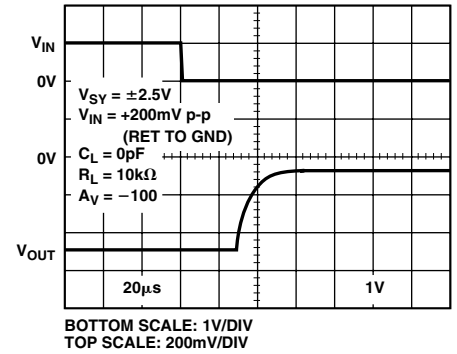


Figure 24. Negative Overvoltage Recovery

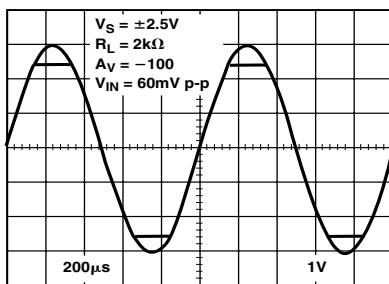


Figure 25. No Phase Reversal

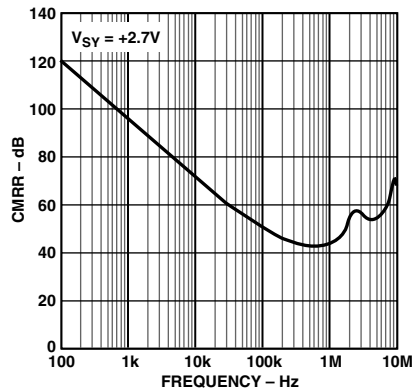


Figure 26. CMRR vs. Frequency at +2.7 V

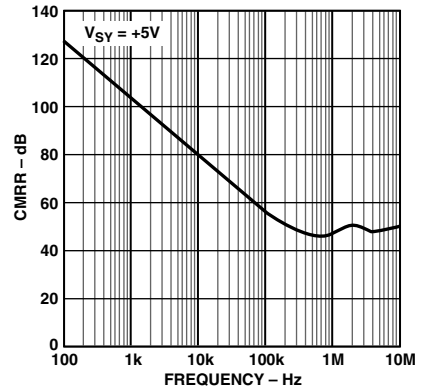


Figure 27. CMRR vs. Frequency at +5 V

AD8551/AD8552/AD8554

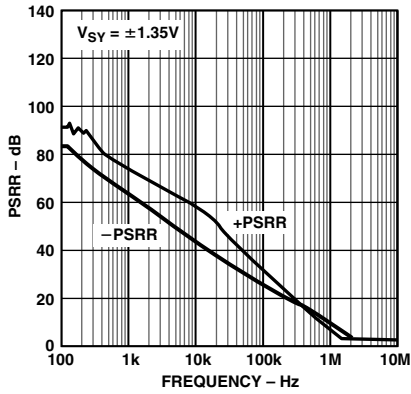


Figure 28. PSRR vs. Frequency at ± 1.35 V

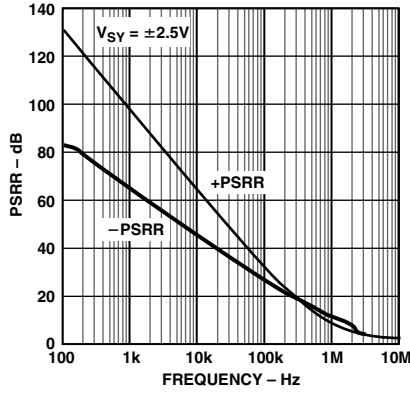


Figure 29. PSRR vs. Frequency at ± 2.5 V

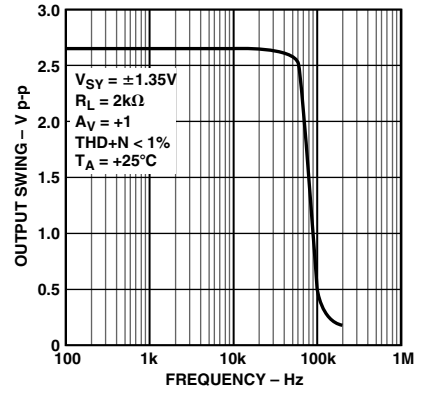


Figure 30. Maximum Output Swing vs. Frequency at +2.7 V

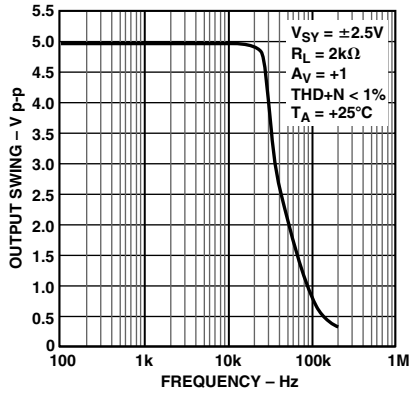


Figure 31. Maximum Output Swing vs. Frequency at +5 V

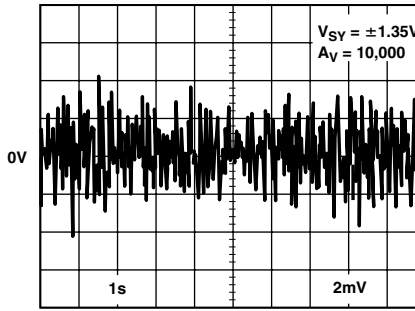


Figure 32. 0.1 Hz to 10 Hz Noise at +2.7 V

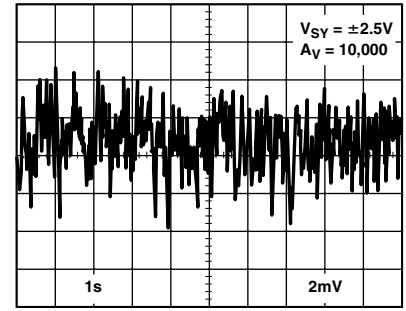


Figure 33. 0.1 Hz to 10 Hz Noise at +5 V

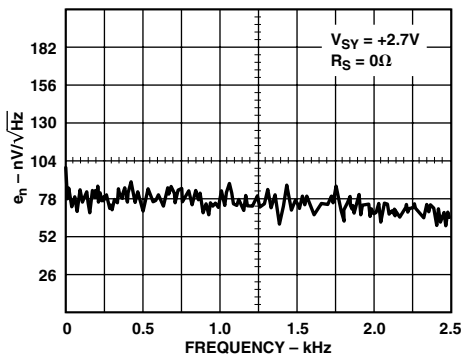


Figure 34. Voltage Noise Density at +2.7 V from 0 Hz to 2.5 kHz

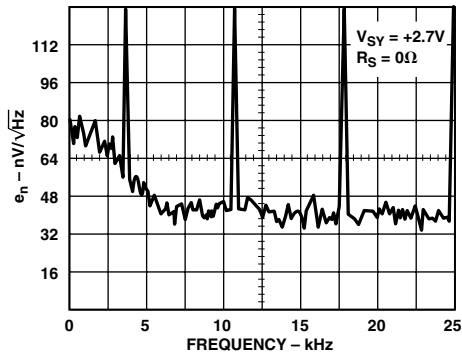


Figure 35. Voltage Noise Density at +2.7 V from 0 Hz to 25 kHz

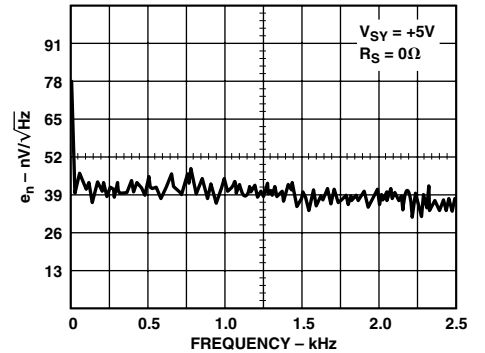


Figure 36. Voltage Noise Density at +5 V from 0 Hz to 2.5 kHz

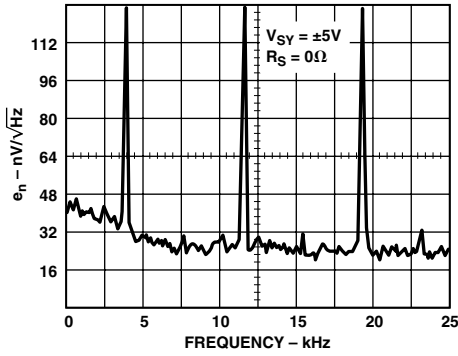


Figure 37. Voltage Noise Density at +5 V from 0 Hz to 25 kHz

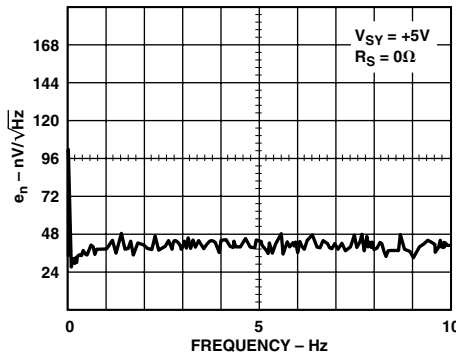


Figure 38. Voltage Noise Density at +5 V from 0 Hz to 10 Hz

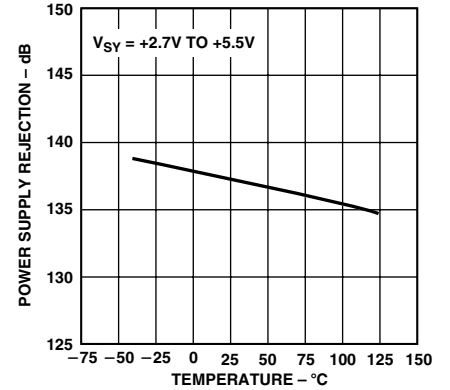


Figure 39. Power-Supply Rejection vs. Temperature

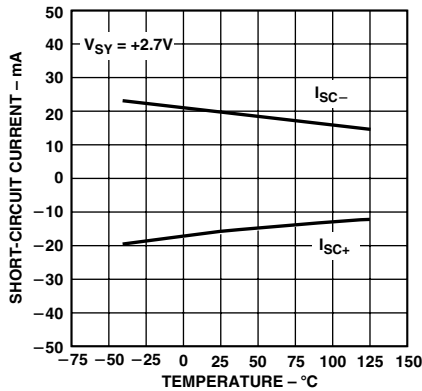


Figure 40. Output Short-Circuit Current vs. Temperature

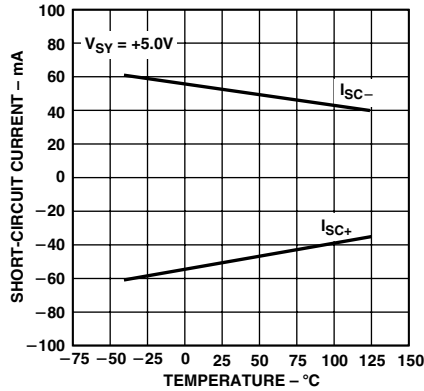


Figure 41. Output Short-Circuit Current vs. Temperature

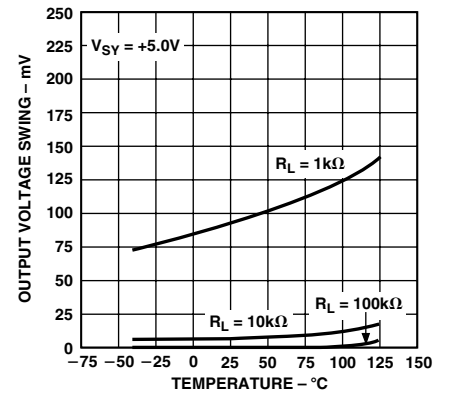


Figure 42. Output Voltage to Supply Rail vs. Temperature

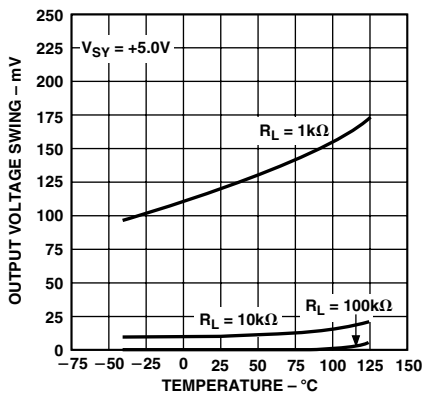


Figure 43. Output Voltage to Supply Rail vs. Temperature

AD8551/AD8552/AD8554

FUNCTIONAL DESCRIPTION

The AD855x family of amplifiers are high precision rail-to-rail operational amplifiers that can be run from a single supply voltage. Their typical offset voltage of less than 1 μV allows these amplifiers to be easily configured for high gains without risk of excessive output voltage errors. The extremely small temperature drift of 5 nV/ $^{\circ}\text{C}$ ensures a minimum of offset voltage error over its entire temperature range of -40°C to $+125^{\circ}\text{C}$, making the AD855x amplifiers ideal for a variety of sensitive measurement applications in harsh operating environments such as under-hood and braking/suspension systems in automobiles.

The AD855x family are CMOS amplifiers and achieve their high degree of precision through autozero stabilization. This autocorrection topology allows the AD855x to maintain its low offset voltage over a wide temperature range and over its operating lifetime.

Amplifier Architecture

Each AD855x op amp consists of two amplifiers, a main amplifier and a secondary amplifier, used to correct the offset voltage of the main amplifier. Both consist of a rail-to-rail input stage, allowing the input common-mode voltage range to reach both supply rails. The input stage consists of an NMOS differential pair operating concurrently with a parallel PMOS differential pair. The outputs from the differential input stages are combined in another gain stage whose output is used to drive a rail-to-rail output stage.

The wide voltage swing of the amplifier is achieved by using two output transistors in a common-source configuration. The output voltage range is limited by the drain to source resistance of these transistors. As the amplifier is required to source or sink more output current, the r_{DS} of these transistors increases, raising the voltage drop across these transistors. Simply put, the output voltage will not swing as close to the rail under heavy output current conditions as it will with light output current. This is a characteristic of all rail-to-rail output amplifiers. Figures 6 and 7 show how close the output voltage can get to the rails with a given output current. The output of the AD855x is short circuit protected to approximately 50 mA of current.

The AD855x amplifiers have exceptional gain, yielding greater than 120 dB of open-loop gain with a load of 2 k Ω . Because the output transistors are configured in a common-source configuration, the gain of the output stage, and thus the open-loop gain of the amplifier, is dependent on the load resistance. Open-loop gain will decrease with smaller load resistances. This is another characteristic of rail-to-rail output amplifiers.

Basic Autozero Amplifier Theory

Autocorrection amplifiers are not a new technology. Various IC implementations have been available for over 15 years and some improvements have been made over time. The AD855x design offers a number of significant performance improvements over older versions while attaining a very substantial reduction in device cost. This section offers a simplified explanation of how the AD855x is able to offer extremely low offset voltages and high open-loop gains.

As noted in the previous section on amplifier architecture, each AD855x op amp contains two internal amplifiers. One is used as the primary amplifier, the other as an autocorrection, or nulling, amplifier. Each amplifier has an associated input offset voltage, which can be modeled as a dc voltage source in series with the noninverting input. In Figures 44 and 45 these are labeled as V_{OSx} , where x denotes the amplifier associated with the offset; A for the nulling amplifier, B for the primary amplifier. The open-loop gain for the +IN and -IN inputs of each amplifier is given as A_x . Both amplifiers also have a third voltage input with an associated open-loop gain of B_x .

There are two modes of operation determined by the action of two sets of switches in the amplifier: An autozero phase and an amplification phase.

Autozero Phase

In this phase, all ϕ_A switches are closed and all ϕ_B switches are opened. Here, the nulling amplifier is taken out of the gain loop by shorting its two inputs together. Of course, there is a degree of offset voltage, shown as V_{OSA} , inherent in the nulling amplifier which maintains a potential difference between the +IN and -IN inputs. The nulling amplifier feedback loop is closed through ϕ_{A2} and V_{OSA} appears at the output of the nulling amp and on C_{M1} , an internal capacitor in the AD855x. Mathematically, we can express this in the time domain as:

$$V_{OA}[t] = A_A V_{OSA}[t] - B_A V_{OA}[t] \quad (1)$$

which can be expressed as,

$$V_{OA}[t] = \frac{A_A V_{OSA}[t]}{1 + B_A} \quad (2)$$

This shows us that the offset voltage of the nulling amplifier times a gain factor appears at the output of the nulling amplifier and thus on the C_{M1} capacitor.

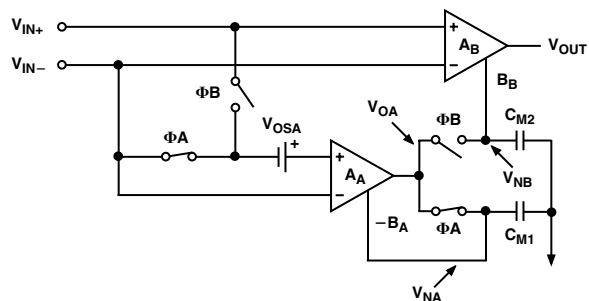


Figure 44. Autozero Phase of the AD855x

Amplification Phase

When the ϕ_B switches close and the ϕ_A switches open for the amplification phase, this offset voltage remains on C_{M1} and essentially corrects any error from the nulling amplifier. The voltage across C_{M1} is designated as V_{NA} . Let us also designate V_{IN} as the potential difference between the two inputs to the primary amplifier, or $V_{IN} = (V_{IN+} - V_{IN-})$. Now the output of the nulling amplifier can be expressed as:

$$V_{OA}[t] = A_A (V_{IN}[t] - V_{OSA}[t]) - B_A V_{NA}[t] \quad (3)$$

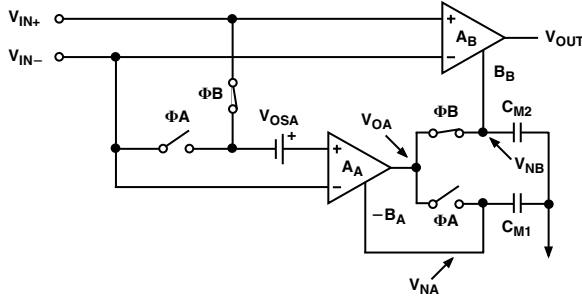


Figure 45. Output Phase of the Amplifier

Because Φ_A is now open and there is no place for C_{M1} to discharge, the voltage V_{NA} at the present time t is equal to the voltage at the output of the nulling amp V_{OA} at the time when Φ_A was closed. If we call the period of the autocorrection switching frequency T_S , then the amplifier switches between phases every $0.5 \times T_S$. Therefore, in the amplification phase:

$$V_{NA}[t] = V_{OA}\left[t - \frac{1}{2}T_S\right] \quad (4)$$

And substituting Equation 4 and Equation 2 into Equation 3 yields:

$$V_{OA}[t] = A_A V_{IN}[t] + A_A V_{OSA}[t] - \frac{A_A B_A V_{OSA}\left[t - \frac{1}{2}T_S\right]}{1 + B_A} \quad (5)$$

For the sake of simplification, let us assume that the autocorrection frequency is much faster than any potential change in V_{OSA} or V_{OSB} . This is a good assumption since changes in offset voltage are a function of temperature variation or long-term wear time, both of which are much slower than the auto-zero clock frequency of the AD855x. This effectively makes V_{OS} time invariant and we can rearrange Equation 5 and rewrite it as:

$$V_{OA}[t] = A_A V_{IN}[t] + \frac{A_A(1 + B_A)V_{OSA} - A_A B_A V_{OSA}}{1 + B_A} \quad (6)$$

or,

$$V_{OA}[t] = A_A \left(V_{IN}[t] + \frac{V_{OSA}}{1 + B_A} \right) \quad (7)$$

We can already get a feel for the autozeroing in action. Note the V_{OS} term is reduced by a $1 + B_A$ factor. This shows how the nulling amplifier has greatly reduced its own offset voltage error even before correcting the primary amplifier. Now the primary amplifier output voltage is the voltage at the output of the AD855x amplifier. It is equal to:

$$V_{OUT}[t] = A_B (V_{IN}[t] + V_{OSB}) + B_B V_{NB} \quad (8)$$

In the amplification phase, $V_{OA} = V_{NB}$, so this can be rewritten as:

$$V_{OUT}[t] = A_B V_{IN}[t] + A_B V_{OSB} + B_B \left[A_A \left(V_{IN}[t] + \frac{V_{OSA}}{1 + B_A} \right) \right] \quad (9)$$

Combining terms,

$$V_{OUT}[t] = V_{IN}[t](A_B + A_B B_B) + \frac{A_A B_A V_{OSA}}{1 + B_A} + A_B V_{OSB} \quad (10)$$

The AD855x architecture is optimized in such a way that $A_A = A_B$ and $B_A = B_B$ and $B_A \gg 1$. Also, the gain product of $A_A B_B$ is much greater than A_B . These allow Equation 10 to be simplified to:

$$V_{OUT}[t] \approx V_{IN}[t] A_A B_A + A_A (V_{OSA} + V_{OSB}) \quad (11)$$

Most obvious is the gain product of both the primary and nulling amplifiers. This $A_A B_A$ term is what gives the AD855x its extremely high open-loop gain. To understand how V_{OSA} and V_{OSB} relate to the overall effective input offset voltage of the complete amplifier, we should set up the generic amplifier equation of:

$$V_{OUT} = k \times (V_{IN} + V_{OS, EFF}) \quad (12)$$

Where k is the open-loop gain of an amplifier and $V_{OS, EFF}$ is its effective offset voltage. Putting Equation 12 into the form of Equation 11 gives us:

$$V_{OUT}[t] \approx V_{IN}[t] A_A B_A + V_{OS, EFF} A_A B_A \quad (13)$$

And from here, it is easy to see that:

$$V_{OS, EFF} \approx \frac{V_{OSA} + V_{OSB}}{B_A} \quad (14)$$

Thus, the offset voltages of both the primary and nulling amplifiers are reduced by the gain factor B_A . This takes a typical input offset voltage from several millivolts down to an effective input offset voltage of submicrovolts. This autocorrection scheme is what makes the AD855x family of amplifiers among the most precise amplifiers in the world.

High Gain, CMRR, PSRR

Common-mode and power supply rejection are indications of the amount of offset voltage an amplifier has as a result of a change in its input common-mode or power supply voltages. As shown in the previous section, the autocorrection architecture of the AD855x allows it to quite effectively minimize offset voltages. The technique also corrects for offset errors caused by common-mode voltage swings and power supply variations. This results in superb CMRR and PSRR figures in excess of 130 dB. Because the autocorrection occurs continuously, these figures can be maintained across the device's entire temperature range, from -40°C to $+125^\circ\text{C}$.

Maximizing Performance Through Proper Layout

To achieve the maximum performance of the extremely high input impedance and low offset voltage of the AD855x, care should be taken in the circuit board layout. The PC board surface must remain clean and free of moisture to avoid leakage currents between adjacent traces. Surface coating of the circuit board will reduce surface moisture and provide a humidity barrier, reducing parasitic resistance on the board. The use of guard rings around the amplifier inputs will further reduce leakage currents. Figure 46 shows how the guard ring should be configured and Figure 47 shows the top view of how a surface mount layout can be arranged. The guard ring does not need to

AD8551/AD8552/AD8554

be a specific width, but it should form a continuous loop around both inputs. By setting the guard ring voltage equal to the voltage at the noninverting input, parasitic capacitance is minimized as well. For further reduction of leakage currents, components can be mounted to the PC board using Teflon standoff insulators.

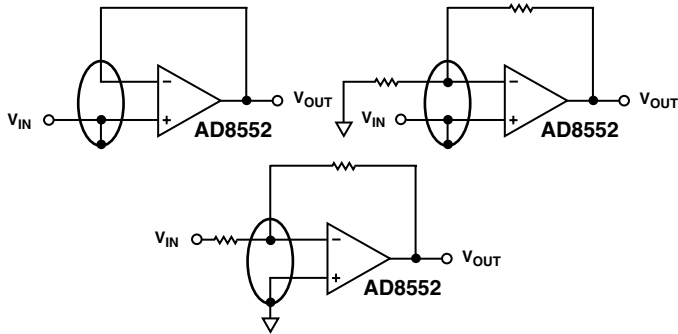


Figure 46. Guard Ring Layout and Connections to Reduce PC Board Leakage Currents

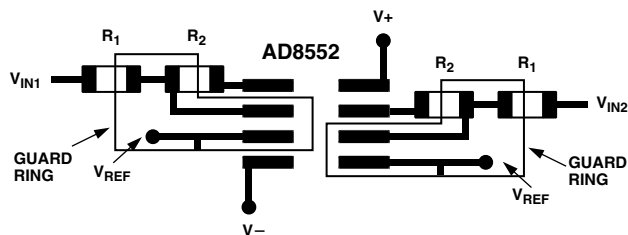


Figure 47. Top View of AD8552 SOIC Layout with Guard Rings

Other potential sources of offset error are thermoelectric voltages on the circuit board. This voltage, also called Seebeck voltage, occurs at the junction of two dissimilar metals and is proportional to the temperature of the junction. The most common metallic junctions on a circuit board are solder-to-board trace and solder-to-component lead. Figure 48 shows a cross-section diagram view of the thermal voltage error sources. If the temperature of the PC board at one end of the component (T_{A1}) is different from the temperature at the other end (T_{A2}), the Seebeck voltages will not be equal, resulting in a thermal voltage error.

This thermocouple error can be reduced by using dummy components to match the thermoelectric error source. Placing the dummy component as close as possible to its partner will ensure both Seebeck voltages are equal, thus canceling the thermocouple error. Maintaining a constant ambient temperature on the circuit board will further reduce this error. The use of a ground plane will help distribute heat throughout the board and will also reduce EMI noise pickup.

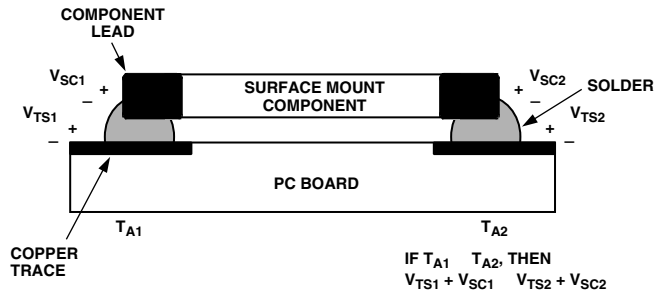
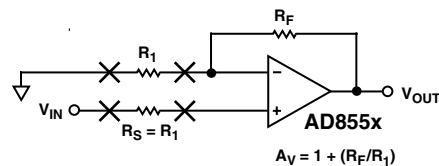


Figure 48. Mismatch in Seebeck Voltages Causes a Thermoelectric Voltage Error



NOTE: R_S SHOULD BE PLACED IN CLOSE PROXIMITY AND ALIGNMENT TO R_1 TO BALANCE SEEBECK VOLTAGES

Figure 49. Using Dummy Components to Cancel Thermoelectric Voltage Errors

1/f Noise Characteristics

Another advantage of autozero amplifiers is their ability to cancel flicker noise. Flicker noise, also known as 1/f noise, is noise inherent in the physics of semiconductor devices and increases 3 dB for every octave decrease in frequency. The 1/f corner frequency of an amplifier is the frequency at which the flicker noise is equal to the broadband noise of the amplifier. At lower frequencies, flicker noise dominates, causing higher degrees of error for sub-Hertz frequencies or dc precision applications.

Because the AD855x amplifiers are self-correcting op amps, they do not have increasing flicker noise at lower frequencies. In essence, low frequency noise is treated as a slowly varying offset error and is greatly reduced as a result of autocorrection. The correction becomes more effective as the noise frequency approaches dc, offsetting the tendency of the noise to increase exponentially as frequency decreases. This allows the AD855x to have lower noise near dc than standard low-noise amplifiers that are susceptible to 1/f noise.

Intermodulation Distortion

The AD855x can be used as a conventional op amp for gain/bandwidth combinations up to 1.5 MHz. The autozero correction frequency of the device is fixed at 4 kHz. Although a trace amount of this frequency will feed through to the output, the amplifier can be used at much higher frequencies. Figure 50 shows the spectral output of the AD8552 with the amplifier configured for unity gain and the input grounded.

The 4 kHz autozero clock frequency appears at the output with less than 2 μ V of amplitude. Harmonics are also present, but at reduced levels from the fundamental autozero clock frequency. The amplitude of the clock frequency feedthrough is proportional to the closed-loop gain of the amplifier. Like other autocorrection amplifiers, at higher gains there will be more clock frequency feedthrough. Figure 51 shows the spectral output with the amplifier configured for a gain of 60 dB.

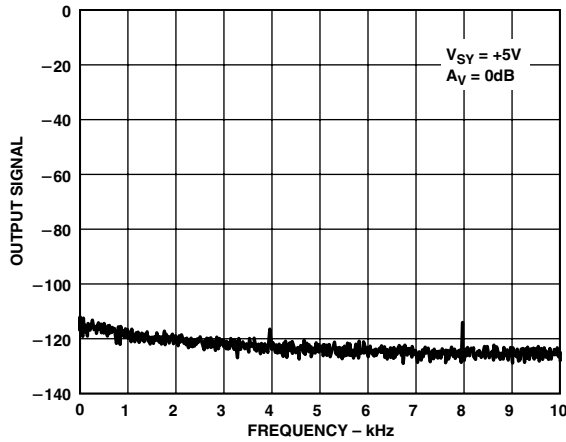


Figure 50. Spectral Analysis of AD855x Output in Unity Gain Configuration

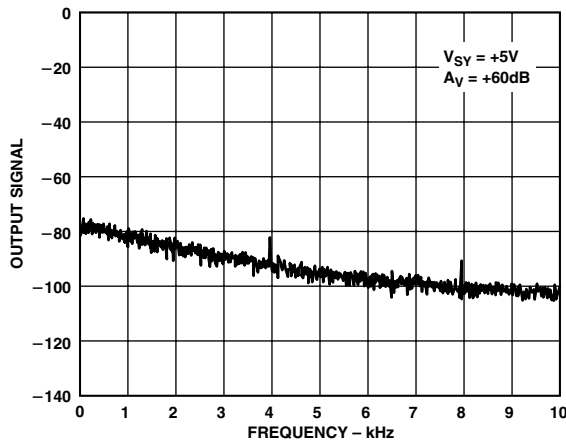


Figure 51. Spectral Analysis of AD855x Output with +60 dB Gain

When an input signal is applied, the output will contain some degree of Intermodulation Distortion (IMD). This is another characteristic feature of all autocorrection amplifiers. IMD will show up as sum and difference frequencies between the input signal and the 4 kHz clock frequency (and its harmonics) and is at a level similar to or less than the clock feedthrough at the output. The IMD is also proportional to the closed loop gain of the amplifier. Figure 52 shows the spectral output of an AD8552 configured as a high gain stage (+60 dB) with a 1 mV input signal applied. The relative levels of all IMD products and harmonic distortion add up to produce an output error of -60 dB relative to the input signal. At unity gain, these would add up to only -120 dB relative to the input signal.

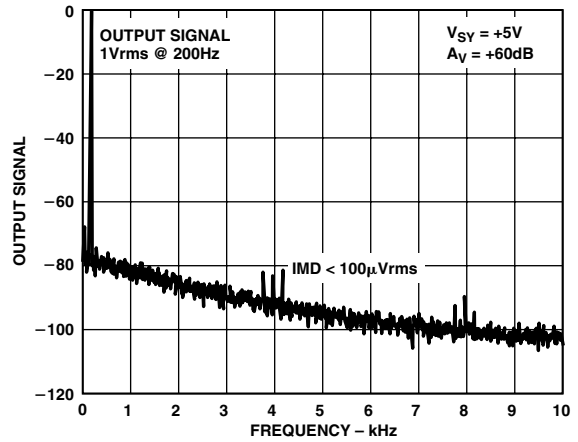


Figure 52. Spectral Analysis of AD855x in High Gain with a 1 mV Input Signal

For most low frequency applications, the small amount of auto-zero clock frequency feedthrough will not affect the precision of the measurement system. Should it be desired, the clock frequency feedthrough can be reduced through the use of a feedback capacitor around the amplifier. However, this will reduce the bandwidth of the amplifier. Figures 53a and 53b show a configuration for reducing the clock feedthrough and the corresponding spectral analysis at the output. The -3 dB bandwidth of this configuration is 480 Hz.

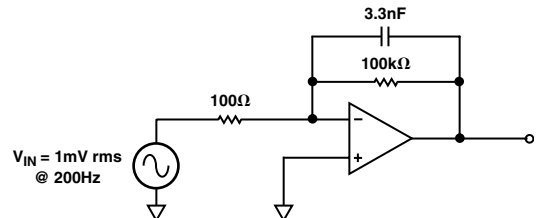


Figure 53a. Reducing Autocorrection Clock Noise with a Feedback Capacitor

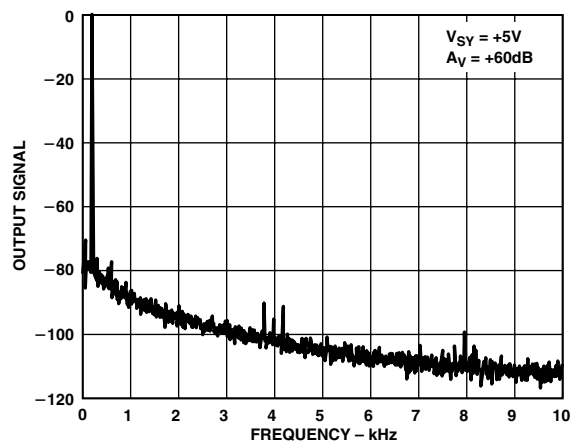


Figure 53b. Spectral Analysis Using a Feedback Capacitor

AD8551/AD8552/AD8554

Broadband and External Resistor Noise Considerations

The total broadband noise output from any amplifier is primarily a function of three types of noise: Input voltage noise from the amplifier, input current noise from the amplifier and Johnson noise from the external resistors used around the amplifier. Input voltage noise, or e_n , is strictly a function of the amplifier used. The Johnson noise from a resistor is a function of the resistance and the temperature. Input current noise, or i_n , creates an equivalent voltage noise proportional to the resistors used around the amplifier. These noise sources are not correlated with each other and their combined noise sums in a root-squared-sum fashion. The full equation is given as:

$$e_{n,TOTAL} = \left[e_n^2 + 4kTr_S + (i_n r_S)^2 \right]^{1/2} \quad (15)$$

Where, e_n = The input voltage noise of the amplifier,
 i_n = The input current noise of the amplifier,
 r_S = Source resistance connected to the noninverting terminal,
 k = Boltzmann's constant (1.38×10^{-23} J/K)
 T = Ambient temperature in Kelvin ($K = 273.15 + ^\circ C$)

The input voltage noise density, e_n of the AD855x is $42 \text{ nV}/\sqrt{\text{Hz}}$, and the input noise, i_n , is $2 \text{ fA}/\sqrt{\text{Hz}}$. The $e_{n,TOTAL}$ will be dominated by input voltage noise provided the source resistance is less than $106 \text{ k}\Omega$. With source resistance greater than $106 \text{ k}\Omega$, the overall noise of the system will be dominated by the Johnson noise of the resistor itself.

Because the input current noise of the AD855x is very small, i_n does not become a dominant term unless r_S is greater than $4 \text{ G}\Omega$, which is an impractical value of source resistance.

The total noise, $e_{n,TOTAL}$, is expressed in volts per square-root Hertz, and the equivalent rms noise over a certain bandwidth can be found as:

$$e_n = e_{n,TOTAL} \times \sqrt{BW} \quad (16)$$

Where BW is the bandwidth of interest in Hertz.

For a complete treatise on circuit noise analysis, please refer to the *1995 Linear Design Seminar* book available from Analog Devices.

Output Overdrive Recovery

The AD855x amplifiers have an excellent overdrive recovery of only $200 \mu\text{s}$ from either supply rail. This characteristic is particularly difficult for autocorrection amplifiers, as the nulling amplifier requires a nontrivial amount of time to error correct the main amplifier back to a valid output. Figure 23 and Figure 24 show the positive and negative overdrive recovery time for the AD855x.

The output overdrive recovery for an autocorrection amplifier is defined as the time it takes for the output to correct to its final voltage from an overload state. It is measured by placing the amplifier in a high gain configuration with an input signal that forces the output voltage to the supply rail. The input voltage is then stepped down to the linear region of the amplifier, usually to half-way between the supplies. The time from the input signal step-down to the output settling to within $100 \mu\text{V}$ of its final value is the overdrive recovery time. Most competitors' autocorrection amplifiers require a number of autozero clock cycles to recover from output overdrive and some can take several milliseconds for the output to settle properly.

Input Overvoltage Protection

Although the AD855x is a rail-to-rail input amplifier, care should be taken to ensure that the potential difference between the inputs does not exceed $+5 \text{ V}$. Under normal operating conditions, the amplifier will correct its output to ensure the two inputs are at the same voltage. However, if the device is configured as a comparator, or is under some unusual operating condition, the input voltages may be forced to different potentials. This could cause excessive current to flow through internal diodes in the AD855x used to protect the input stage against overvoltage.

If either input exceeds either supply rail by more than 0.3 V , large amounts of current will begin to flow through the ESD protection diodes in the amplifier. These diodes are connected between the inputs and each supply rail to protect the input transistors against an electrostatic discharge event and are normally reverse-biased. However, if the input voltage exceeds the supply voltage, these ESD diodes will become forward-biased. Without current limiting, excessive amounts of current could flow through these diodes causing permanent damage to the device. If inputs are subject to overvoltage, appropriate series resistors should be inserted to limit the diode current to less than 2 mA maximum.

Output Phase Reversal

Output phase reversal occurs in some amplifiers when the input common-mode voltage range is exceeded. As common-mode voltage is moved outside of the common-mode range, the outputs of these amplifiers will suddenly jump in the opposite direction to the supply rail. This is the result of the differential input pair shutting down, causing a radical shifting of internal voltages which results in the erratic output behavior.

The AD855x amplifier has been carefully designed to prevent any output phase reversal, provided both inputs are maintained within the supply voltages. If one or both inputs could exceed either supply voltage, a resistor should be placed in series with the input to limit the current to less than 2 mA . This will ensure the output will not reverse its phase.

Capacitive Load Drive

The AD855x has excellent capacitive load driving capabilities and can safely drive up to 10 nF from a single $+5 \text{ V}$ supply. Although the device is stable, capacitive loading will limit the bandwidth of the amplifier. Capacitive loads will also increase the amount of overshoot and ringing at the output. An R-C snubber network, Figure 54, can be used to compensate the amplifier against capacitive load ringing and overshoot.

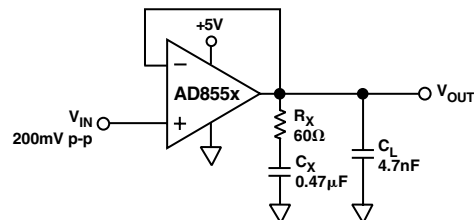


Figure 54. Snubber Network Configuration for Driving Capacitive Loads

Although the snubber will not recover the loss of amplifier bandwidth from the load capacitance, it will allow the amplifier to drive larger values of capacitance while maintaining a minimum of overshoot and ringing. Figure 55 shows the output of an AD855x driving a 1 nF capacitor with and without a snubber network.

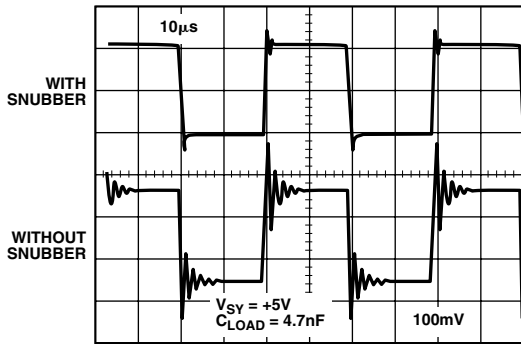


Figure 55. Overshoot and Ringing are Substantially Reduced Using a Snubber Network

The optimum value for the resistor and capacitor is a function of the load capacitance and is best determined empirically since actual C_{LOAD} will include stray capacitances and may differ substantially from the nominal capacitive load. Table I shows some snubber network values that can be used as starting points.

Table I. Snubber Network Values for Driving Capacitive Loads

C_{LOAD}	R_X	C_X
1 nF	200 Ω	1 nF
4.7 nF	60 Ω	0.47 μ F
10 nF	20 Ω	10 μ F

Power-Up Behavior

On power-up, the AD855x will settle to a valid output within 5 μ s. Figure 56a shows an oscilloscope photo of the output of the amplifier along with the power supply voltage, and Figure 56b shows the test circuit. With the amplifier configured for unity gain, the device takes approximately 5 μ s to settle to its final output voltage. This turn-on response time is much faster than most other auto-correction amplifiers, which can take hundreds of microseconds or longer for their output to settle.

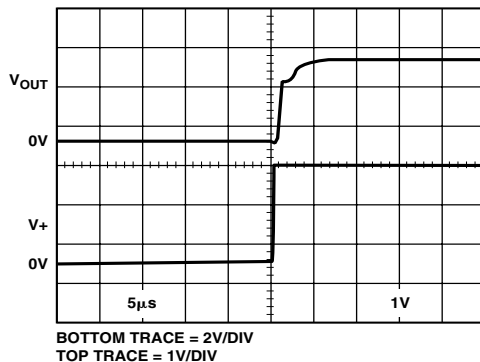


Figure 56a. AD855x Output Behavior on Power-Up

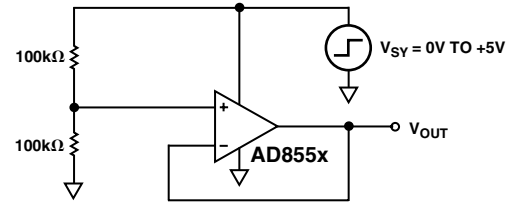


Figure 56b. AD855x Test Circuit for Turn-On Time

APPLICATIONS

A +5 V Precision Strain-Gage Circuit

The extremely low offset voltage of the AD8552 makes it an ideal amplifier for any application requiring accuracy with high gains, such as a weigh scale or strain-gage. Figure 57 shows a configuration for a single supply, precision strain-gage measurement system.

A REF192 provides a +2.5 V precision reference voltage for A2. The A2 amplifier boosts this voltage to provide a +4.0 V reference for the top of the strain-gage resistor bridge. Q1 provides the current drive for the 350 Ω bridge network. A1 is used to amplify the output of the bridge with the full-scale output voltage equal to:

$$V_{OUT} = \frac{2 \times (R_1 + R_2)}{R_B} \quad (17)$$

Where R_B is the resistance of the load cell. Using the values given in Figure 57, the output voltage will linearly vary from 0 V with no strain to +4.0 V under full strain.

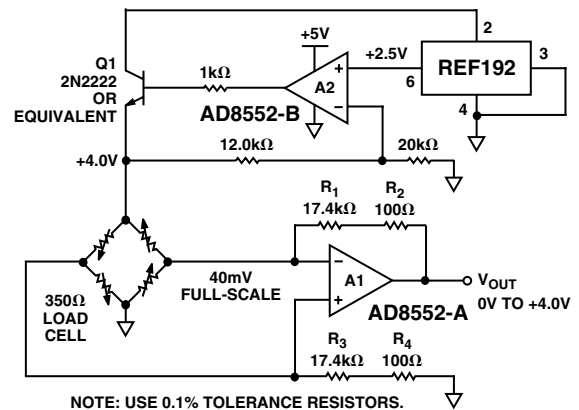


Figure 57. A +5 V Precision Strain-Gage Amplifier

+3 V Instrumentation Amplifier

The high common-mode rejection, high open-loop gain, and operation down to +3 V of supply voltage makes the AD855x an excellent choice of op amp for discrete single supply instrumentation amplifiers. The common-mode rejection ratio of the AD855x is greater than 120 dB, but the CMRR of the system is also a function of the external resistor tolerances. The gain of the difference amplifier shown in Figure 58 is given as:

$$V_{OUT} = V1 \left(\frac{R_4}{R_3 + R_4} \right) \left(1 + \frac{R_1}{R_2} \right) - V2 \left(\frac{R_2}{R_1} \right) \quad (18)$$

AD8551/AD8552/AD8554

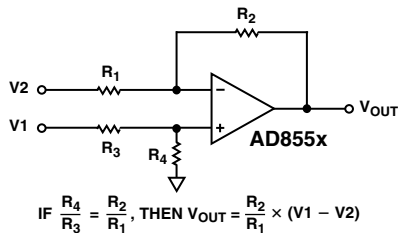


Figure 58. Using the AD855x as a Difference Amplifier

In an ideal difference amplifier, the ratio of the resistors are set exactly equal to:

$$A_V = \frac{R_2}{R_1} = \frac{R_4}{R_3} \quad (19)$$

Which sets the output voltage of the system to:

$$V_{OUT} = A_V(V1 - V2) \quad (20)$$

Due to finite component tolerance the ratio between the four resistors will not be exactly equal, and any mismatch results in a reduction of common-mode rejection from the system. Referring to Figure 58, the exact common-mode rejection ratio can be expressed as:

$$CMRR = \frac{R_1 R_4 + 2R_2 R_4 + R_2 R_3}{2R_1 R_4 - 2R_2 R_3} \quad (21)$$

In the 3 op amp instrumentation amplifier configuration shown in Figure 59, the output difference amplifier is set to unity gain with all four resistors equal in value. If the tolerance of the resistors used in the circuit is given as δ , the worst-case CMRR of the instrumentation amplifier will be:

$$CMRR_{MIN} = \frac{1}{2\delta} \quad (22)$$

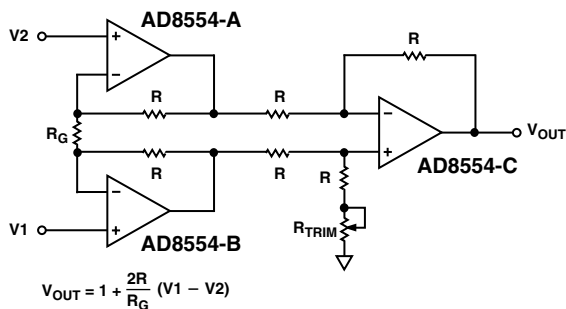


Figure 59. A Discrete Instrumentation Amplifier Configuration

Thus, using 1% tolerance resistors would result in a worst-case system CMRR of 0.02, or 34 dB. Therefore either high precision resistors or an additional trimming resistor, as shown in Figure 59, should be used to achieve high common-mode rejection. The value of this trimming resistor should be equal to the value of R multiplied by its tolerance. For example, using 10 k Ω resistors with 1% tolerance would require a series trimming resistor equal to 100 Ω .

A High Accuracy Thermocouple Amplifier

Figure 60 shows a K-type thermocouple amplifier configuration with cold-junction compensation. Even from a +5 V supply, the AD8551 can provide enough accuracy to achieve a resolution of better than 0.02°C from 0°C to 500°C. D1 is used as a temperature measuring device to correct the cold-junction error from the thermocouple and should be placed as close as possible to the two terminating junctions. With the thermocouple measuring tip immersed in a zero-degree ice bath, R_6 should be adjusted until the output is at 0 V.

Using the values shown in Figure 60, the output voltage will track temperature at 10 mV/°C. For a wider range of temperature measurement, R_9 can be decreased to 62 k Ω . This will create a 5 mV/°C change at the output, allowing measurements of up to 1000°C.

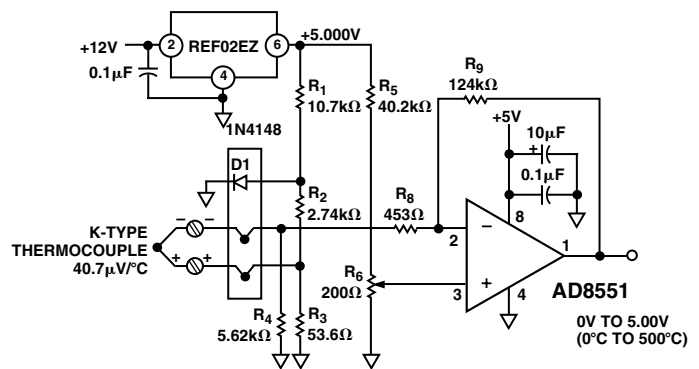


Figure 60. A Precision K-Type Thermocouple Amplifier with Cold-Junction Compensation

Precision Current Meter

Because of its low input bias current and superb offset voltage at single supply voltages, the AD855x is an excellent amplifier for precision current monitoring. Its rail-to-rail input allows the amplifier to be used as either a high-side or low-side current monitor. Using both amplifiers in the AD8552 provides a simple method to monitor both current supply and return paths for load or fault detection.

Figure 61 shows a high-side current monitor configuration. Here, the input common-mode voltage of the amplifier will be at or near the positive supply voltage. The amplifier's rail-to-rail input provides a precise measurement even with the input common-mode voltage at the supply voltage. The CMOS input structure does not draw any input bias current, ensuring a minimum of measurement error.

The 0.1 Ω resistor creates a voltage drop to the noninverting input of the AD855x. The amplifier's output is corrected until this voltage appears at the inverting input. This creates a current through R_1 , which in turn flows through R_2 . The Monitor Output is given by:

$$\text{Monitor Output} = R_2 \times \left(\frac{R_{SENSE}}{R_1} \right) \times I_L \quad (23)$$

Using the components shown in Figure 61, the Monitor Output transfer function is 2.5 V/A.

Figure 62 shows the low-side monitor equivalent. In this circuit, the input common-mode voltage to the AD8552 will be at or near ground. Again, a 0.1 Ω resistor provides a voltage drop proportional to the return current. The output voltage is given as:

$$V_{OUT} = V + \left(\frac{R_2}{R_1} \times R_{SENSE} \times I_L \right) \quad (24)$$

For the component values shown in Figure 62, the output transfer function decreases from V+ at -2.5 V/A.

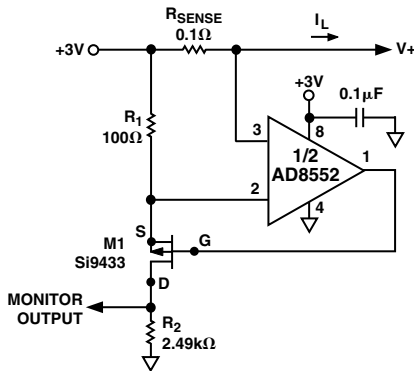


Figure 61. A High-Side Load Current Monitor

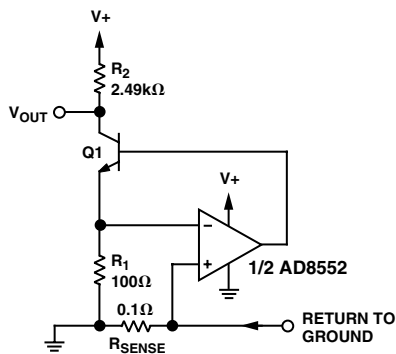


Figure 62. A Low-Side Load Current Monitor

Precision Voltage Comparator

The AD855x can be operated open-loop and used as a precision comparator. The AD855x has less than 50 μV of offset voltage when run in this configuration. The slight increase of offset voltage stems from the fact that the autocorrection architecture operates with lowest offset in a closed loop configuration, that is, one with negative feedback. With 50 mV of overdrive, the device has a propagation delay of 15 μs on the rising edge and 8 μs on the falling edge.

Care should be taken to ensure the maximum differential voltage of the device is not exceeded. For more information, please refer to the section on Input Overvoltage Protection.

SPICE Model

The SPICE macro-model for the AD855x amplifier is given in Listing 1. This model simulates the typical specifications for the AD855x, and it can be downloaded from the Analog Devices website at <http://www.analog.com>. The schematic of the macro-model is shown in Figure 63.

Transistors M1 through M4 simulate the rail-to-rail input differential pairs in the AD855x amplifier. The EOS voltage source in series with the noninverting input establishes not only the 1 μV offset voltage, but is also used to establish common-mode and power supply rejection ratios and input voltage noise. The differential voltages from nodes 14 to 16 and nodes 17 to 18 are reflected to E1, which is used to simulate a secondary pole-zero combination in the open-loop gain of the amplifier.

The voltage at node 32 is then reflected to G1, which adds an additional gain stage and, in conjunction with CF, establishes the slew rate of the model at 0.5 V/μs. M5 and M6 are in a common-source configuration, similar to the output stage of the AD855x amplifier. EG1 and EG2 fix the quiescent current in these two transistors at 100 μA, and also help accurately simulate the V_{OUT} vs. I_{OUT} characteristic of the amplifier.

The network around ECM1 creates the common-mode voltage error, with CCM1 setting the corner frequency for the CMRR roll-off. The power supply rejection error is created by the network around EPS1, with CPS3 establishing the corner frequency for the PSRR roll-off. The two current loops around nodes 80 and 81 are used to create a 42 nV/√Hz noise figure across RN2. All three of these error sources are reflected to the input of the op amp model through EOS. Finally, GSY is used to accurately model the supply current versus supply voltage increase in the AD855x.

This macro-model has been designed to accurately simulate a number of specifications exhibited by the AD855x amplifier, and is one of the most true-to-life macro-models available for any op amp. It is optimized for operation at +27°C. Although the model will function at different temperatures, it may lose accuracy with respect to the actual behavior of the AD855x.

AD8551/AD8552/AD8554

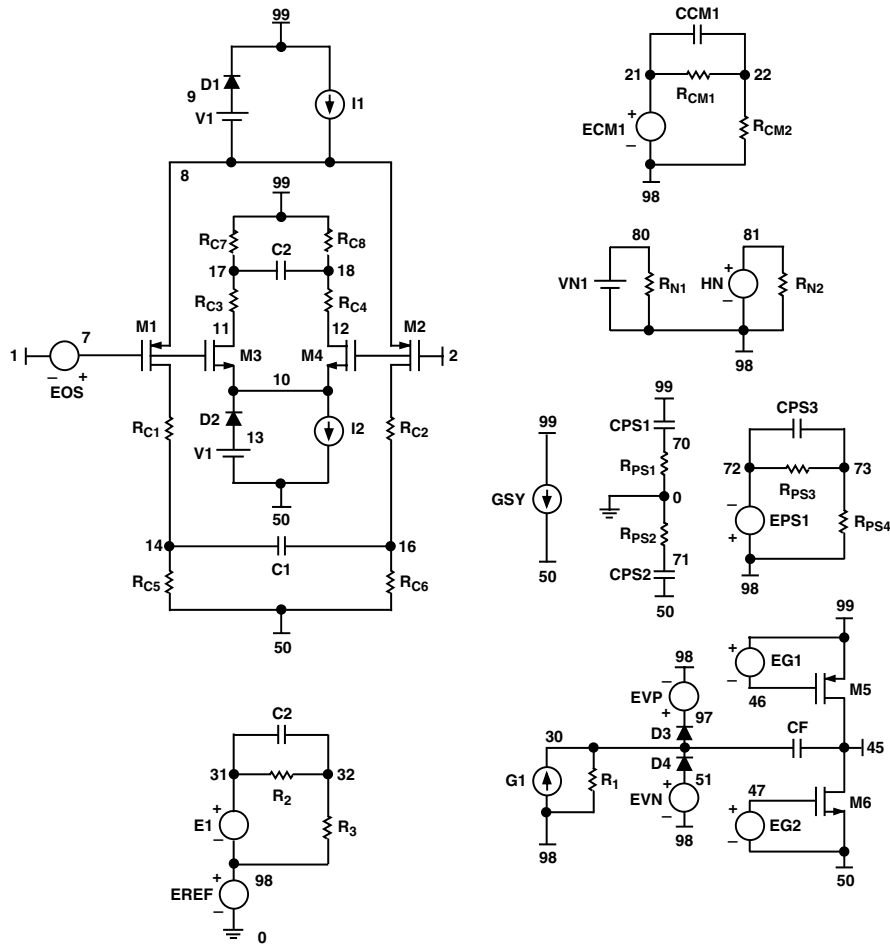


Figure 63. Schematic of the AD855x SPICE Macro-Model

SPICE macro-model for the AD855x

```

* AD8552 SPICE Macro-model
* Typical Values
* 7/99, Ver. 1.0
* TAM / ADSC
*
* Copyright 1999 by Analog Devices
*
* Refer to "README.DOC" file for License
* Statement. Use of this model indicates
* your acceptance of the terms and
* provisions in the License Statement.
*
* Node Assignments
*
*           noninverting input
*           |   inverting input
*           |   |   positive supply
*           |   |   |   negative supply
*           |   |   |   |   output
*           |   |   |   |   |
*.SUBCKT AD8552 1 2 99 50 45
*
* INPUT STAGE
*
M1  4  7  8  8 PIX L=1E-6 W=355.3E-6
M2  6  2  8  8 PIX L=1E-6 W=355.3E-6
M3 11  7 10 10 NIX L=1E-6 W=355.3E-6
M4 12  2 10 10 NIX L=1E-6 W=355.3E-6
RC1  4 14 9E+3
RC2  6 16 9E+3
RC3 17 11 9E+3
RC4 18 12 9E+3
RC5 14 50 1E+3
RC6 16 50 1E+3
RC7 99 17 1E+3
RC8 99 18 1E+3
C1  14 16 30E-12
C2  17 18 30E-12
I1  99  8 100E-6
I2  10 50 100E-6
V1  99  9 0.3
V2  13 50 0.3
D1  8  9 DX
D2  13 10 DX
EOS  7  1 POLY(3) (22,98) (73,98) (81,98)
+ 1E-6 1 1 1
IOS  1  2 2.5E-12
*
* CMRR 120dB, ZERO AT 20Hz
*
ECM1 21 98 POLY(2) (1,98) (2,98) 0 .5 .5
RCM1 21 22 50E+6
CCM1 21 22 159E-12
RCM2 22 98 50
*
* PSRR=120dB, ZERO AT 1Hz
*
RPS1 70  0 1E+6
RPS2 71  0 1E+6
CPS1 99 70 1E-5
CPS2 50 71 1E-5
EPSY 98 72 POLY(2) (70,0) (0,71) 0 1 1
RPS3 72 73 15.9E+6
CPS3 72 73 10E-9
RPS4 73 98 16

```

```

* VOLTAGE NOISE REFERENCE OF 42nV/rt(Hz)
*
VN1 80 98 0
RN1 80 98 16.45E-3
HN  81 98 VN1 42
RN2 81 98 1
*
* INTERNAL VOLTAGE REFERENCE
*
EREF 98  0 POLY(2) (99,0) (50,0) 0 .5 .5
GSY  99 50 (99,50) 48E-6
EVP  97 98 (99,50) 0.5
EVN  51 98 (50,99) 0.5
*
* LHP ZERO AT 7MHz, POLE AT 50MHz
*
E1 32 98 POLY(2) (4,6) (11,12) 0 .5814 .5814
R2 32 33 3.7E+3
R3 33 98 22.74E+3
C3 32 33 1E-12
*
* GAIN STAGE
*
G1 98 30 (33,98) 22.7E-6
R1 30 98 259.1E+6
CF 45 30 45.4E-12
D3 30 97 DX
D4 51 30 DX
*
* OUTPUT STAGE
*
M5  45 46 99 99 POX L=1E-6 W=1.111E-3
M6  45 47 50 50 NOX L=1E-6 W=1.6E-3
EG1 99 46 POLY(1) (98,30) 1.1936 1
EG2 47 50 POLY(1) (30,98) 1.2324 1
*
* MODELS
*
.MODEL POX PMOS (LEVEL=2,KP=10E-6,
+ VTO=-1,LAMBDA=0.001,RD=8)
.MODEL NOX NMOS (LEVEL=2,KP=10E-6,
+ VTO=1,LAMBDA=0.001,RD=5)
.MODEL PIX PMOS (LEVEL=2,KP=100E-6,
+ VTO=-1,LAMBDA=0.01)
.MODEL NIX NMOS (LEVEL=2,KP=100E-6,
+ VTO=1,LAMBDA=0.01)
.MODEL DX D(IS=1E-14,RS=5)
.ENDS AD8552

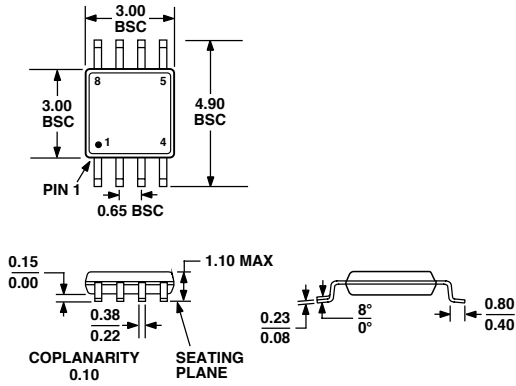
```

AD8551/AD8552/AD8554

OUTLINE DIMENSIONS

8-Lead MSOP Package [MSOP] (RM-8)

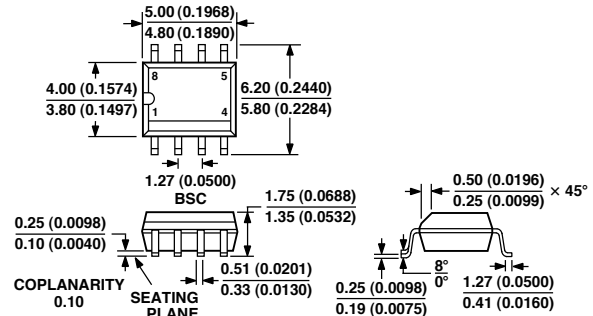
Dimensions shown in millimeters



COMPLIANT TO JEDEC STANDARDS MO-187AA

8-Lead Standard Small Outline Package [SOIC] Narrow Body (RN-8)

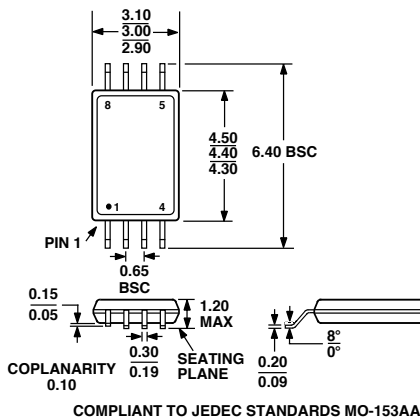
Dimensions shown in millimeters and (inches)



COMPLIANT TO JEDEC STANDARDS MS-012AA
CONTROLLING DIMENSIONS ARE IN MILLIMETERS; INCH DIMENSIONS (IN PARENTHESES) ARE ROUNDED-OFF MILLIMETER EQUIVALENTS FOR REFERENCE ONLY AND ARE NOT APPROPRIATE FOR USE IN DESIGN

8-Lead Thin Shrink Small Outline Package [TSSOP] (RU-8)

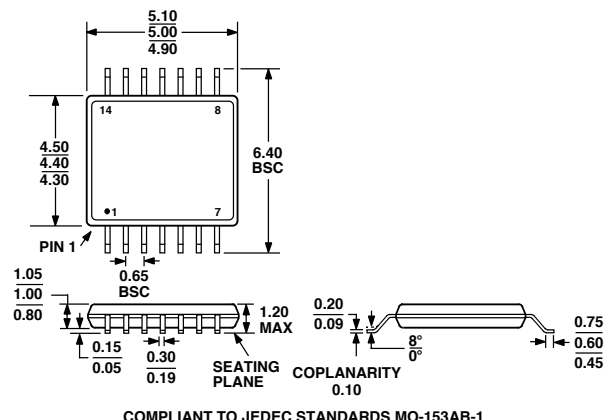
Dimensions shown in millimeters



COMPLIANT TO JEDEC STANDARDS MO-153AA

14-Lead Thin Shrink Small Outline Package [TSSOP] (RU-14)

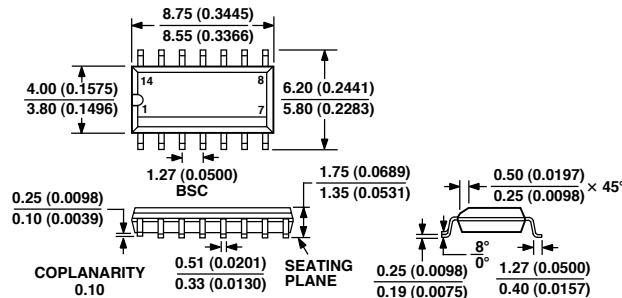
Dimensions shown in millimeters



COMPLIANT TO JEDEC STANDARDS MO-153AB-1

14-Lead Standard Small Outline Package [SOIC] Narrow Body (RN-8)

Dimensions shown in millimeters and (inches)



CONTROLLING DIMENSIONS ARE IN MILLIMETERS; INCH DIMENSIONS (IN PARENTHESES) ARE ROUNDED-OFF MILLIMETER EQUIVALENTS FOR REFERENCE ONLY AND ARE NOT APPROPRIATE FOR USE IN DESIGN

Revision History

Location

Page

11/02—Data Sheet changed from REV. 0 to REV. A.

Edits to Figure 60 16

Updated OUTLINE DIMENSIONS 20